OSU ILLIAD TN#: 275031

Journal Title: Applied ocean research.
Volume: 13
Issue: 1
Month/Year: 1991
Pages: 2-11

ILL Number: 36969670

Article Author:
Article Title: Niedzwecki, J.M., Thampi, S.K.; Snap loading in Marine cable systems

Borrower: MFL

Borrower: MFL
Lending String: *ORE,RIN,FQR,UAF,SEA

Ariel: 192.190.45.28

Patron: Hobson, Brett
Maxcost: $20IFM

Fax: (831)632-4403

This item will be invoiced at the end of the month

OCLC Number: 4648153

Photocopy/Loan/Invoice/Postage Charges: **Reciprocal - No Char**

Shipping Address:
CSU MOSS LANDING MARINE LABS
LIBRARY, ILL
8272 MOSS LANDING ROAD
MOSS LANDING, CA 95039

Oregon State University
ILL -- Phone: (541) 737-7311 Email: valley.ill@oregonstate.edu Fax: (541) 737-1328 Ariel: 128.193.162.52

Snap loading of Marine cable systems

JOHN M. NIEDZWECKI

Department of Civil Engineering, Texas A & M University, College Station, TX 77843-3136 USA

SREEKUMAR K. THAMPI

GE/Houston, 1050 Bay Area Boulevard, Houston, TX 77058 USA

This study presents a general two-part analysis procedure for the investigation of snap load behavior of marine cable systems in regular seas. A simple dynamic model of a package suspended from a multi-cable configuration is presented. It is used as the basis to develop dimensionless curves which are useful for the preliminary assessment of the susceptibility of a design to snap load behavior. For cases where this model indicates a strong possibility of snap load behavior, the designer must use a more complex dynamic model. A deepwater marine cable system, similar to that designed for scientific coring studies of the Mid-Atlantic Ridge, is used as the basis for the illustrative examples. The packages to be placed on the seafloor had complicated geometrical shapes with openings through which fluid could pass. Experiments to determine the hydrodynamic added-mass were performed and the results compared to common hydrodynamic approximations. The numerical examples illustrate the sensitivity of these dynamic response predictions to hydrodynamic approximations, ship heading and design wave conditions. They also show that it may be possible to avoid snap loading through proper design, and that if snap loading occurs it is possible to mitigate its effects without complete failure of the system.

Key Words: Marine cables, dynamics response, model tests, offshore engineering, marine cable systems, snap loading.

INTRODUCTION

Marine cable systems are used in a wide variety of offshore operations. These include the deployment and recovery of instrumentation packages, salvage operations, underwater construction, scientific deep ocean coring studies and deep ocean mining activities. These systems utilize wire rope, chain or synthetic rope, and are sometimes used in combination with slender pipe sections. The cable portions are configured with either single or multiple lines depending upon the particular application. Successful operation in the ocean environment of these marine cable systems is dependent upon the proper selection of system components, which when assembled can sustain the anticipated loading developed through the motion of the vessel and subsea package. The dominant excitation is assumed to be the heaving of the vessel as it responds to the seaway. The marine cable system is assumed to maintain its initial orientation without rotation during its response to the heave excitation. This assumption is generally correct except when the payload is in the zone of surface wave action, subjected to strong sub-sea currents, or when the cable configuration or package design results in excessive transverse movement. In those cases one should consider the need to model combined axial and transverse dynamics of the cable/package system. This study focuses exclusively upon the vertical heave response behavior associated with the lowering and raising of large packages to the seafloor in regular seas.

An accurate means of predicting line tensions, accounting for the transition between taut and slack line conditions, is required for the proper design of marine cable systems. As the amplitude and frequency of excitation increases, compressive loads from the oscillatory dynamic component may exceed static tensile loads. A cable is flexible and cannot resist compressive loads. Thus, under any compressive loading conditions a cable becomes slack. Depending upon the rate of subsequent re-tensioning, the cable can experience a severe impact load, which is referred to as snap loading. Snap loads can be several orders larger than the normal static and dynamic loading and are the dominant design consideration when known to exist. Because of the strong non-linear nature of the snap phenomenon, which is characterized by a sudden loss of cable stiffness in the slack regime, time domain simulations are the most practical means of predicting snap loads.

Analytical and experimental investigation of snap loads in stranded steel cables were carried out by Goeller and Laura[1] using a lumped, single-degree-of-freedom (SDOF) model. Segmented cables with viscoelastic properties were also considered. Liu[2] used a two-dimensional, multi-degree-of-freedom (MDOF) model to determine snap loads in lifting and mooring lines. Later,

Paper accepted September 1989. Discussion closes August 1991.

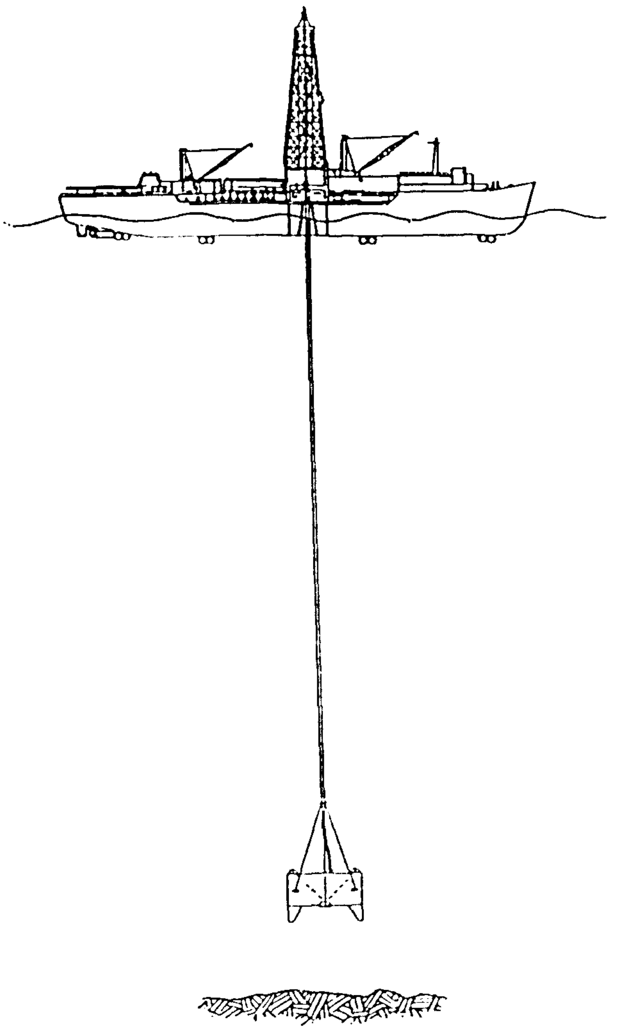

Fig. 1. A sketch of a drillship lowering a hard rock guide base to the seafloor

Yoshida and Oka[3] studied snap loads in taut moored platforms through model tests and theoretical analysis. The present study was motivated by the deep ocean coring activities of the Ocean Drilling Program (ODP), whose mission is the scientific study of the geological history of ocean basins[4]. These coring activities often require the placement of large packages on the ocean floor. The marine cable system used to lower a hard rock guide base to the seafloor is depicted in Fig. 1. The hard rock guide base was designed to facilitate drilling into the mid-Atlantic ridge. As can be seen, the hard rock guide base is suspended by three cables from the bottom of a drill string and lowered from a dynamically positioned drillship. Engineering data on the drillship, riserless drill pipe systems, and related package designs can be found in a recent article by Niedzwecki and Harding[5]. Some additional details on the geometry of the hard rock guide base and another package, a re-entry cone, are provided in Fig. 2. This deepwater system must be designed to insure that neither the breaking strength of the cable system nor the capacity of the various drill string components are exceeded during placement or recovery operations.

This study begins with the examination of a single-degree-of-freedom model of a cable/package system. Critical dimensionless ratios are identified and design curves developed for predicting taut and slack cable conditions. When the SDOF model suggests that slack cable conditions will probably occur, a multi-degree-of-freedom-model of the complete drillstring cable package system is needed. One type of MDOF model which is suitable for describing marine cable systems is presented. By performing the numerical simulation of snap loads in the time domain, the non-linear terms in the equations of motion can be handled directly without equivalent linearization. A discussion of the non-linearities which must be considered for this type of problem have been previously presented by Niedzwecki and Thampi[6]. The primary sources of non-linearity in this study are the subsea package damping and the cable stiffness.

Hydrodynamic data needed to model the two packages, which involve porus complex geometrical shapes, is not available in the literature. Therefore a series of small scale model tests were performed to determine the adequacy of hydrodynamic approximations which have been used extensively in the past. Accurate knowledge of the hydrodynamic added-mass is needed because the snap load response predictions are very sensitive to small changes in the virtual mass. The experimental procedure is described and comparisons with several analytical predictions based upon standard hydrodynamic models are presented.

There are two major issues which must be addressed in the design process. First, it is necessary to determine whether snap loading will occur for a particular cable configuration given a specific design wave environment. Secondly, if snap loading is expected to occur, the severity of the snap loading must be estimated. The first issue is addressed in this article through the development of the design curves which provide an initial indication of the snap load potential of a particular design. The second issue requires a more detailed simulation and the recognition of the fact that some level of repeated snap loading can be tolerated by the marine cable system. The major parameters of concern and the non-linear response behavior are examined in the illustrative examples presented in this study. The methodology developed in this study is quite general and can be easily interpreted for non-marine applications.

SDOF SNAP LOAD MODEL

As a first approximation, consider a single-degree-of-freedom model of the cable and package system. The excitation can be modified to provide for a number of interpretations regarding its source. Consider a vertical, elastic cable suspending a large package in a quiescent fluid, subject to harmonic excitation at the suspension point. This can be represented by the linearized equation of motion

$$M_v \frac{d^2x}{dt^2} + C\frac{dx}{dt} + K_c x = K_c X_0 \sin \omega t \tag{1}$$

where, M_v is the virtual mass which represents the sum of the structural mass of the package and the associated hydrodynamic added mass, C is the hydrodynamic damping coefficient, K_c represents the bi-linear axial stiffness of the cable or cable system, X_0 is the excitation amplitude, ω is the frequency of the excitation and, x is the displacement of the package. A convenient approximation that can be used to estimate the hydrodynamic damping

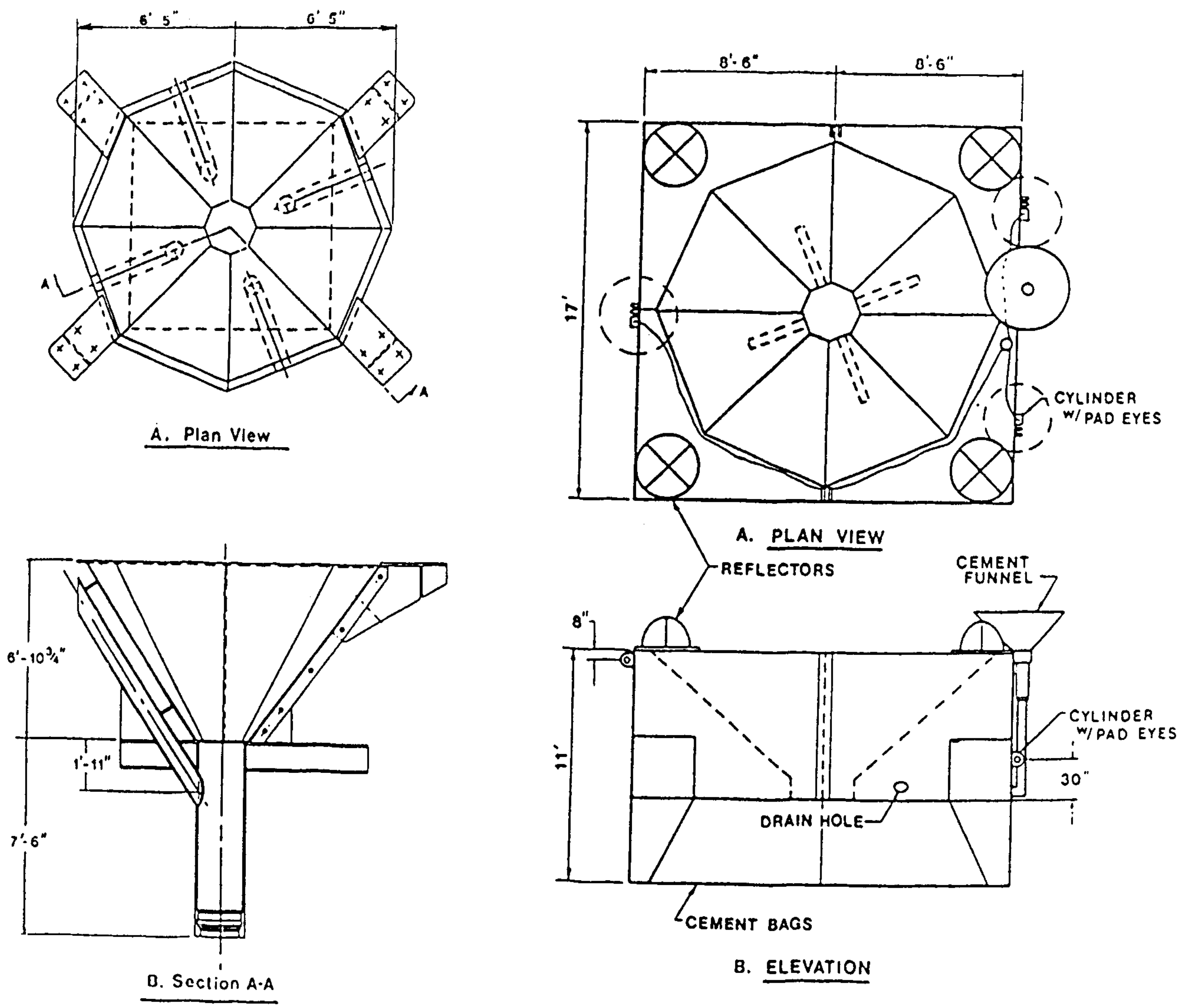

Fig. 2. Definition sketch: a.) Re-entry cone assembly, b.) Hard rock guide base assembly

coefficient for the SDOF model can be derived based on equal energy dissipation considerations[7]. It can be expressed as

$$C \simeq (4\omega/3\pi)\rho C_d A_p X \tag{2}$$

where, ρ is the fluid mass density, C_d is the viscous drag coefficient, A_p is the cross-sectional area of the package projected in the direction of motion and X is the amplitude of the steady state response. For a taut cable or cable system, the axial stiffness can be expressed as

$$K_c = A_c E_c / L_c \tag{3}$$

where, A_c represents the effective cross-sectional area of the cable, which is less than the area computed based upon the cable diameter because of its weave, E_c is the elastic modulus of the cable material and L_c is the cable length. These variables can also be interpreted to represent a cable system made up of several cables provided that they are assigned equivalent values. The steady state solutions for the amplitude and phase of the response are

$$X = \frac{X_0}{\sqrt{(1-\Lambda^2)^2 + (2\xi\Lambda)^2}} \tag{4}$$

$$\theta = \tan^{-1}\left(\frac{2\xi\Lambda}{1-\Lambda^2}\right) \tag{5}$$

where,

$$\Lambda = \omega/(\sqrt{K_c/M_v}) \tag{6}$$

$$\xi = C/(2\sqrt{K_c M_v}) \tag{7}$$

Here, θ is the phase of the steady state response, Λ is the dimensionless frequency ratio and, ξ is the dimensionless damping ratio. It is assumed that during the motion of the system, the cable system remains vertical and the orientation of the package does not change. The mass and damping associated with the cable system are assumed to be negligible. The solution is obtained with the further assumption that K_c is a positive constant, which is valid only for taut cables. In the event of a slack condition this solution is no longer valid. This occurs when

$$X_0 \sin(\omega t) - X \sin(\omega t - \theta) \geq X_{st} \tag{8}$$

where, X_{st} is the static stretch of the cable system. Dividing through by X_0 and substituting for X from the steady state solution, one obtains another form of equation (8).

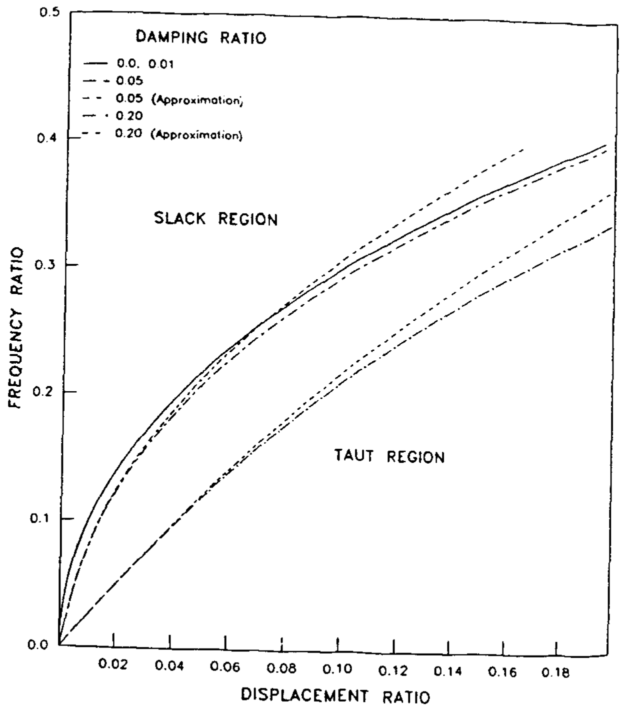

Fig. 3. Dimensionless curve for prediction of slack cable conditions for small values of displacement and frequency ratios

The instant at which the left hand side of this equation is a maximum is obtained by differentiating it with respect to time, setting the derivative equal to zero and, then confirming that the second derivative at that instant is negative. Substituting the resulting expression for time into equation (8), introducing several trigonometric identities, rearranging and introducing the dimensionless variables Λ and, ξ one finally obtains

$$\frac{\Lambda^4+(2\xi\Lambda)^2}{\sqrt{\Lambda^4(\Lambda^2+4\xi^2-1)^2+(2\xi\Lambda)^2}}\geq\tau \tag{9}$$

where

$$\tau=X_{st}/X_0 \tag{10}$$

Here, τ is the dimensionless displacement ratio. Equation (9) is the condition for impending slack in the cable or cable system. Stated in this form, it can be observed that the initiation of slack in the cable or cables depends collectively on three dimensionless variables and not individually on the various parameters that constitute these groups.

The separation of slack and taut regions, as expressed through the use of equation (9), are shown graphically in Figs 3 and 4. Figure 3 presents results for a small portion of the range of equation (9) and Fig. 4 presents a much broader range. Both figures include limiting cases for comparative reasons. For small values of the damping ratio, $\xi<0.01$, damping can be neglected and equation (9) can be well approximated by the expression

$$\frac{\Lambda^2}{|1-\Lambda^2|}=\tau \tag{11}$$

In Fig. 3, the curves for $\xi=0$ and $\xi=0.01$ are seen to be virtually identical. Further, for small displacement ratios, $\tau<0.04$, equation (9) can be approximated as

$$\sqrt{\Lambda^4+(2\xi\Lambda)^2}=\tau \tag{12}$$

This approximation is presented as dashed curves in Fig. 3 for values of $\xi=0.05$ and $\xi=0.20$.

The delineation of slack and taut regions is shown for a broad range of frequency, displacement and damping ratios in Fig. 4. The curves are asymptotic to the line $\tau=1.0$ and reach a peak value when Λ is close to unity. For the undamped system the displacement ratio goes to infinity at a frequency ratio of unity. As the damping ratio increases, the corresponding values of the peak displacement ratios decrease and tend to occur at frequency ratios greater than unity. The curves shown in Fig. 4, have a common point of intersection at frequency ratio of $1/\sqrt{2}$ and a displacement ratio of unity. Based upon these curves, three observations can be made. First, for values of displacement ratio less than unity, the transition from taut to slack region occurs at frequency ratios less than $1/\sqrt{2}$. This observation is consistent with the conclusion of Goeller and Laura[8], that excitation frequencies well below the resonant frequency can initiate slackness in the cable system. For any displacement ratio less than one, it is possible to exit the slack region only by reducing the frequency ratio. Secondly, there is a maximum displacement ratio corresponding to any specified damping ratio beyond which the cable always remains taut. Finally, for displacement ratios greater than unity but less than the maximum value, there is a range of frequency ratios which can cause slackness in the cable. In this case, it is possible to get through the slack region by increasing the frequency ratio.

MDOF SNAP LOAD MODEL

To better understand the response of marine cable systems predicted by the SDOF model to be susceptible to snap load behavior, a multi-degree-of-freedom system representation is needed. The drill string can be divided into a series of elements which can be modelled as either

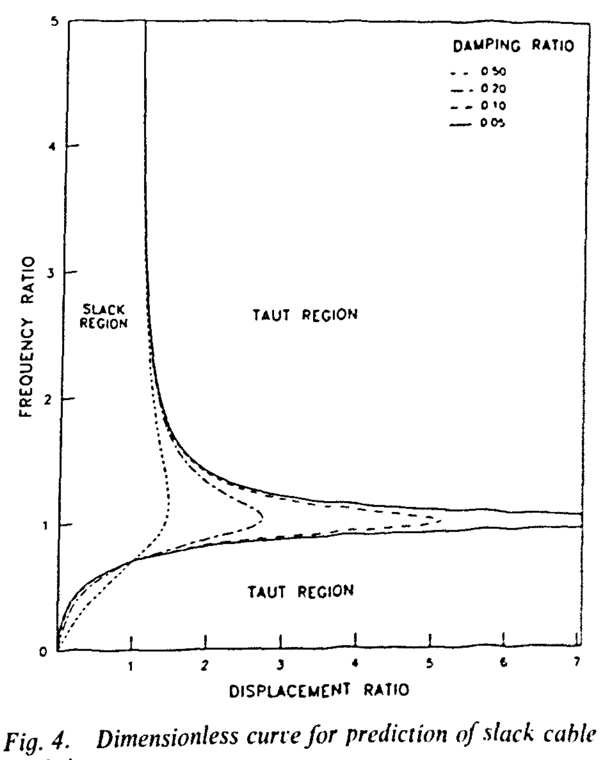

Fig. 4. Dimensionless curve for prediction of slack cable conditions

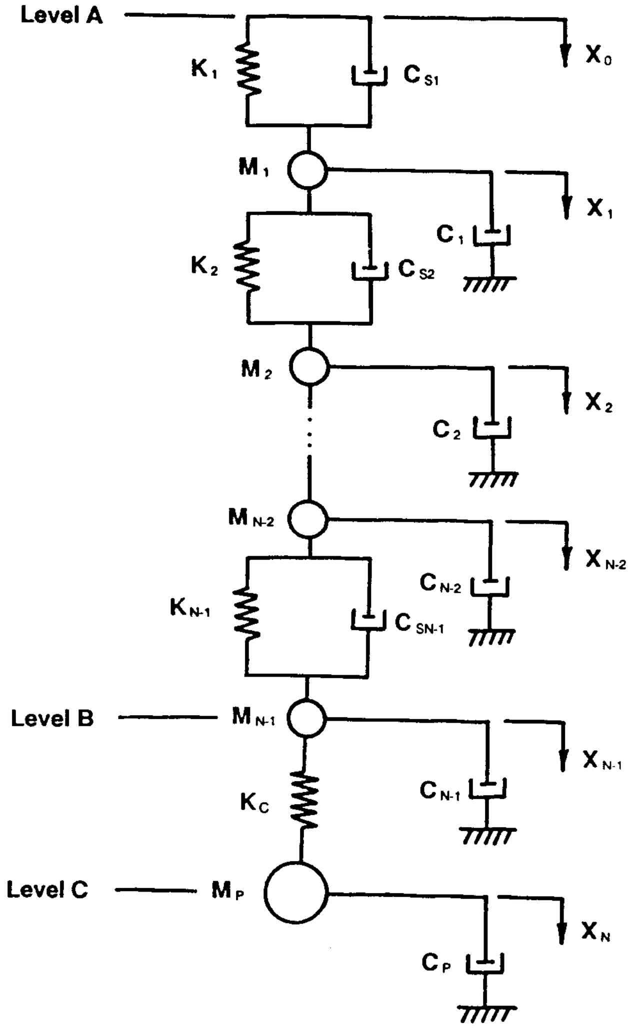

Fig. 5. A dynamic model of the marine cable system shown in Fig. 1

discrete[9] or continuous segments[6]. For the discrete lumped parameter model, shown in Fig. 5, the mass of each element along with the hydrodynamic added mass and any fluid mass entrapped within the drill string element, is concentrated at the bottom of each model element. The hydrodynamic added mass contribution arises from step changes in drill string geometry due to the inclusion of tool joints and rubbers. For many applications these contributions are negligible when compared to the structural mass[10]. Each model element is assumed to have constant geometric and elastic properties although, for deepwater systems a variety of pipe sizes are used and these values will vary over the length of the pipe system. The system damping includes both structural and hydrodynamic damping. The linearized structural damping coefficient is a function of the logarithmic decrement of the drill string material and the excitation frequency[11]. Hydrodynamic damping contributions arise from skin friction along the drill string and from flow separation caused by geometric discontinuities[6]. As in the case of the SDOF system, the cable was modelled as a bi-linear spring and the mass and damping contributions of the cable were assumed to be negligible.

The equations of motion for the discrete system, shown in Fig. 5, are developed by considering the force balance at each model node. The resulting system of differential equations

$$
\begin{aligned}
&M_{v1}\frac{d^2x_1}{dt^2}+(C_{s1}+C_{s2}+C_1)\frac{dx_1}{dt}-C_{s2}\frac{dx_2}{dt}\\
&\qquad+(K_1+K_2)x_1-K_2x_2=C_{s1}\frac{dx_0}{dt}+K_1x_0\\
&M_{v2}\frac{d^2x_2}{dt^2}-C_{s2}\frac{dx_1}{dt}+(C_{s2}+C_{s3}+C_2)\frac{dx_2}{dt}-C_{s3}\frac{dx_3}{dt}\\
&\qquad-K_2x_1+(K_2+K_3)x_2-K_3x_3=0\\
&\vdots\\
&M_{VN-1}\frac{d^2x_{N-1}}{dt^2}-C_{SN-1}\frac{dx_{N-2}}{dt}+(C_{SN-1}+C_{N-1})\frac{dx_{N-1}}{dt}\\
&\qquad-K_{N-1}K_{N-2}+(K_{N-1}+K_C)x_{N-1}\\
&\qquad-K_Cx_N=0\\
&M_{VN}\frac{d^2x_N}{dt^2}+C_p\frac{dx_N}{dt}-K_Cx_{N-1}+K_Cx_N=W-K_CX_{st}
\end{aligned}
\tag{13}
$$

where,

$$C_p=\tfrac{1}{2}C_d\rho A_p\left|\frac{dx_N}{dt}\right| \tag{14}$$

and, C_{si} is the structural damping coefficient of the i^{th} element, C_i is the hydrodynamic damping coefficient of the i^{th} element and, W is the submerged weight of the package. Additional details can be found in the Deep Sea Drilling Report[11]. When this system of coupled equations is arranged in matrix form, it becomes evident that the mass matrix is diagonal and the damping and stiffness matrices are tri-diagonal. Recognizing this form can improve the computational algorithms used in the numerical simulations.

The excitation at the top of the drill string is caused by the heaving motion of the drillship under the action of monochromatic waves. The response of the ship is characterized by its heave response amplitude operators (RAOs'), which are a function of wave frequency and ship heading. As is typical, computer generated RAOs' for a typical drillship were used in this study. The excitation at the top of the drillstring can be expressed as

$$x_0(t)=\frac{H}{2}\,\mathrm{RAO}(\omega,\phi)\sin\omega t \tag{15}$$

where H is the incident wave height, ω is the wave frequency, and ϕ is the ship heading.

The matrix equations of motion were solved in the time domain using the Newmark Beta method[12]. For time domain simulations in which steady state response is the primary objective, the initial conditions specified must be realistic in order to avoid very large transient periods. These transients can dominate the dynamic response for lightly damped systems. Techniques to accelerate decay of the transient response were used in the computations presented later in this article[13]. After each time step, the cable is checked to determine if it has become slack. This is done by comparing its instantaneous length to its unstretched length, i.e. $x_{N-1}-x_N>X_{st}$. The package hydrodynamic drag contribution is also updated after each time step, and the current values of K_c and C_p are used to compute the effective stiffness matrix.

Integration proceeds until some specified time interval is attained.

EVALUATION OF HYDRODYNAMIC PROPERTIES

Analytical results of the preceding section indicate that the occurrence of snap in cables is controlled by three variables Λ, ξ and τ. The main sources of uncertainty in evaluating these variables are the modulus of elasticity of the cable line, the added-mass and the drag of the payload. The modulus of elasticity is usually specified by the cable manufacturer. The drag coefficient and the added-mass of non-classical shaped subsea packages can be determined accurately only through laboratory tests. Drag coefficient values typically vary from 0.5 to 2.0, depending on the shape of the payload and ambient flow conditions. For the hard rock guide base and cable system considered in this study, this results in ξ values ranging from about 0.0002 to 0.01. From Fig. 4 it can be observed that for the hard rock guide base configuration, snap conditions are not sensitive to ξ values in this range and hence, experimental determination of drag coefficient is not warranted. This conclusion may not be valid for other systems with smaller values of package mass and cable stiffness.

The added-mass of the subsea package depends on the shape of the body and, in this case, flow conditions through the package. For regular solid shapes like spheres, cylinders and rectangular blocks, the equations for computing the added-mass are well established[14]. However, for complicated geometrical shapes like the hard rock guide base, idealizations using these classical formulae are difficult to justify. In this study, the added-mass was evaluated experimentally by vibrating scale models through resonance both in air and in water. The corresponding shift in the natural frequencies was then used to infer the hydrodynamic added-mass. Specifically

$$m_a = [(f_a/f_w)^2 - 1]m \qquad (16)$$

where, m_a is the hydrodynamic added-mass, m is the structural mass, f_a is the resonant frequency in air and, f_w is the resonant frequency in water.

The scale models used in the laboratory tests were mounted at the bottom of a cantilevered Plexiglass cylinder fastened through a support structure to a two-dimensional wave tank. The models were attached by means of a mounting pin which facilitated the proper orientation of the model and a small feedback accelerometer. The excitation force was applied horizontally a small distance below the top of the cylinder. The frequency of the input force was programmed to sweep between set limits at constant amplitude. The frequency limits were chosen so as to include the resonance frequencies, at which point the displacement amplitudes are maximum. A second check on the resonance conditions was made by displaying the input force and the output displacement signals simultaneously on an oscilloscope. At resonance, a 90 degree phase difference between the input force and response displacement can be expected.

Results from the model tests are shown in Table 1. These include data for a rectangular block, a circular disk, two re-entry cone models and, two hard rock guide base models. The first two models were included in order to validate the testing procedure and establish error estimates. The theoretical and semi-empirical predictions for hydrodynamic added-mass are presented in column 4 marked theory[14]. The last column provides an estimate of the error between the experimental hydrodynamic added-mass and that predicted using the various approximations. It is normalized with respect to the predictions based upon theory and here positive values indicate an under prediction by theory. The experimental results for the circular disk and the rectangular block are in good agreement with the commonly used predictive equations. Until recently, these models have been used to approximate the hydrodynamic added-mass of the re-entry cone and hard rock guide base, shown in Fig. 4. The re-entry cone can be thought of as a large funnel through which water can easily flow. The smaller scale model, as shown in Table 1, has a 38% difference in m_a. As the model scale increases the deviation seems to increase. This may be due in part to the fact that the smaller model restricts the flow through it. For the hard rock guide base, the deviation appears to decrease as the model scale increases. These results are preliminary and, although the trends seem reasonable, more experimental data is needed since these bodies are radically different from those presented in the current literature. The small scale model tests clearly demonstrated that the use of the idealized models to predict the hydrodynamic added-mass was not an entirely satisfactory approach. This is a critical issue, because small differences in estimates of the hydrodynamic added-mass can significantly influence the snap load characteristics of a marine cable design.

ILLUSTRATIVE EXAMPLES

The numerical examples presented in this section illustrate the use of the dimensionless curves, generated using the simple dynamic model, and the use of a more complex dynamic model for time domain simulations. A drillstring configuration similar to that used by the Ocean Drilling Program was selected as the basis for the numerical examples which follow[9]. As illustrated in Fig. 1, the drillstring is used in combination with three cables for the deployment of a hard rock guide base in very deep water. An 8000 ft steel drill pipe system was selected. The drill string consists of 2600 ft of 5.5 in outside diameter (OD) drill pipe, nearest the drillship, connected to 5400 ft of 5.0 inch OD drill pipe. The dry weight per unit length of the drill pipe used is 32 lbs/ft for the 5.5 in pipe and 22 lbs/ft for the 5.0 in pipe. At the bottom of the drillstring,

Table 1. Theoretical and experimental hydrodynamic added-mass values

Model	Scale	Mass	Hydrodynamic Added Mass		
		(gm)	Theory (gm)	Experiment (gm)	Difference (%)
(1)	(2)	(3)	(4)	(5)	(6)
Rectangular Block	1:61	157	394	402	2
Circular Disk	1:61	47	96	102	6
Re-entry Cone	1:61	96	96	132	38
Re-entry Cone	1:34	340	547	853	56
Hard Rock Base	1:61	123	394	535	36
Hard Rock Base	1:34	666	2244	2658	18

a hard rock guide base is attached by a cable system utilizing three steel cables. As shown in Fig. 2, the hard rock guide base is quite large and has an estimated dry weight of 40250 lbs. Based upon the experimental results, presented earlier, the virtual mass was estimated to be 9570 slugs. Based upon the results of the SDOF model, a drag coefficient of 1.0 was assumed for this simulation. To study the effect of varying the cable stiffness, two cable systems were selected and they are referred to as system A and system B. System A consists of three 1.5 in diameter steel cables with a vertical projected height of 75 ft, an effective cross-sectional area of 4 sq in and an equivalent axial stiffness of 1.33×10^6 lbs/ft. System B consists of three 1.75 in diameter steel cables with a vertical projected height of 50 ft, an effective cross-sectional area of 5.45 sq in and an equivalent axial stiffness of 2.73×10^6 lbs/ft. The mass and damping contribution of these systems were neglected since they were deemed negligible compared to the contributions of the package.

SDOF EXAMPLES

A summary of the SDOF estimates for three different cases is presented in Table 2. Two cable systems were analyzed to determine whether the cables would remain taut or experience slack cable conditions, indicating the onset of snap loads. The information needed for this analysis included the expected wave height and corresponding wave period, the cable system configuration, specifically the geometric configuration, the cable sizes and material properties, basic information about the package and, some information on the vessel RAOs' in heave as a function of heading. If the vessel data is not available, simple engineering estimates can be used. Based upon this information, the corresponding values of the frequency ratio, the displacement ratio and damping ratio can be computed. Using these dimensionless values a determination of whether the system is in the taut or slack regime can be made using Fig. 3 or Fig. 4. If the results indicate that the design is in or close to the slack regime and changes to the original design do not significantly change the results, one must use a more complex dynamic simulation model to study the system design in more detail.

For case 1, a wave height of 12 ft, a wave period of 8 s and a ship heading of 0 degrees was selected. Both systems, A and B, remained in the taut regime. In order to illustrate the effect of slight changes in the ocean wave environment, the wave period was varied in Case 2 and as can be seen system A moved into the slack regime. A realistic vessel RAO was used and as a result the displacement at the top of the cable system increased significantly. Thus, depending on the vessel RAOs', small changes in the environmental data can result in the cable system moving from the taut to the slack regime.

Variation of the cable stiffness was found to have only a minimal effect on the state of the cable system. This can be explained in terms of a power series expansion of equation (11)

$$\Lambda^2(1+\Lambda^2+\ldots)=\tau \tag{17}$$

which is valid for frequency ratios less than unity. For small values of Λ, the higher order terms in the expansion can be neglected. Further expanding equation (17) in terms of its primitive variables shows that the cable stiffness occurs in the denominator on both sides of the equation. Therefore its variation has very little influence on the sate of the cable system. For larger values of the frequency ratio higher order terms in the expansion become more significant. This implies that by increasing the cable stiffness, the system will tend to move away from the slack regime and the possibility of snap loads will decrease. However, the magnitude of the snap loads, when they do occur, will be significantly greater for stiffer cable systems than for softer systems[8]. It can also be seen from equation (17) that a more effective way of avoiding snap load conditions is to increase the ratio of the structural mass to the virtual mass, i.e. M_p/M_v. This can be achieved by using high density payloads and/or altering the package geometry to reduce the added-mass contributions. The effect of this variation is shown in Table 2, Case 2.

The effect of varying the ships heading on snap load predictions is illustrated in Case 3. For the same wave environment as in Case 1, a change in heading from 0 to 90 degrees results in a significant increase in the excitation amplitude on the top of the cable system. This is due to the higher RAOs' associated with the beam sea conditions. Both cable systems are now in the slack regime. Thus, one can conclude that changes in vessel orientation can be used effectively to mitigate snap load conditions.

Table 2. Prediction of slack and taut conditions for marine cable systems

Case (1)	Ocean Environment (2)	Cable System (3)	M_p/M_v (4)	Λ (5)	τ (6)	ξ (7)	Regime (8)
1	H = 12 ft T = 8 s $\phi = 0°$ X_o = 2.5 ft	A B	0.13 0.13	0.0665 0.0465	0.0105 0.0051	0.0021 0.0015	Taut Taut
2	H = 12 ft T = 7 s $\phi = 0°$ X_o = 4.5 ft	A A	0.13 0.143	0.0761 0.0727	0.0058 0.0058	0.0044 0.0046	Slack Taut
3	H = 12 ft T = 8 s $\phi = 90°$ X_o = 10 ft	A B	0.13 0.13	0.0665 0.0465	0.0026 0.0013	0.0085 0.0060	Slack Slack

MDOF EXAMPLES

Time domain simulations were carried out using a MDOF model of the drill string and cable system A. The results for the three cases, summarized in Table 2, are presented in Figs 6, 7 and 8. Referring to Fig. 5, they include: 1) the displacement time series at the top of the drill string (level A), 2) the displacement time series at the bottom of the drill string (level B), 3) the displacement time series at the package (level C) and, 4) the cable system tension time series.

Case 1 was selected because, based upon the SDOF analysis, not snap load behavior was expected. As shown in Fig. 6, snap loads do not occur and the steady state responses appear to be sinusoidal with very little distortion from the non-linear damping. The troughs represent the upward motion and the crests correspond to the downward motion. The peak tension in the cables is slightly in excess of 50,000 lbs, which is within the range of the normal working loads for the cable system.

Case 2 was selected since, the SDOF model indicated that the cable system could be susceptible to snap load

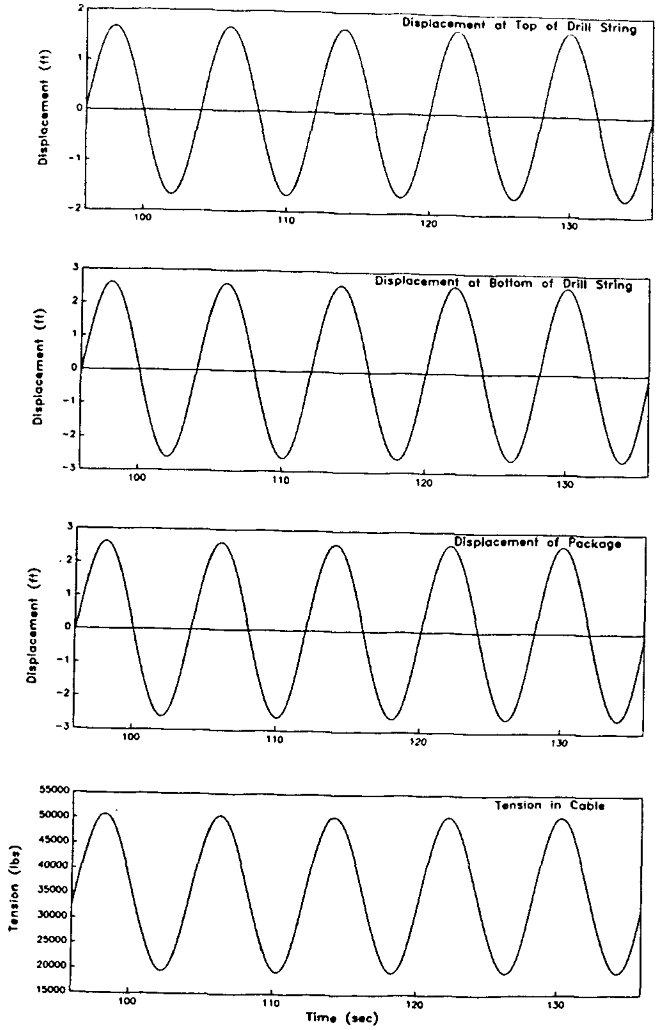

Fig. 6. Time series simulation for case 1, system A, where no snap loads occur

behavior. The MDOF simulation results for case 2 are presented in Fig. 7. As can be seen snap loading did occur but, was of low severity. In this non-linear coupled system, the displacement at level B can be interpreted as the result of the excitation introduced by the heaving of the vessel (level A) and the motion of the package (level C). Initially, the drillstring and the package move together on a downward path. The cables go slack during the ascent of the system and this occurs at the first trough. While the system is in this slack regime the coupling is lost and the drillstring responds independently. At the next trough, the cables re-engage and the snap load occurs. As can be seen from the predicted tension in the cables, the tension levels continue to oscillate as the system attempts to stabilize. The peak value of these oscillations can be greater than that of the initial snap load.

Case 3 was selected since, the SDOF model indicated that the cable system would exhibit snap load behavior. The MDOF simulation results for Case 3 are presented in Fig. 8. For this case, the excitation of the system is significantly increased due to the re-orientation of the surface vessel. Again, the cables go slack during the system ascent, with the slack initiation occurring at the deepest troughs. Re-engagement of the cables and snap loading occur at the second shallow trough within each cycle. The effects of non-linearities can be seen quite clearly, as the cable stiffness comes into play. The package motion is characterized by flat troughs and sharp crests. The tension level behavior is similar to that of Case 2, but much more severe in magnitude. No break strength of other failure criteria were employed in these simulations, thus the response behavior is cyclic even at these severe loads. The cable tensions shown exceed 110,000 lbs and 250,000 lbs respectively, which is still less than the estimated breaking strength of the cable system. However, the ability of the cable system to sustain repeated snap loading will be reduced as the magnitude of the snap loads increases. The examples presented here are for moderate sea conditions. For more severe sea conditions, snap loads can be expected to easily exceed the breaking strength of the cable system.

SUMMARY AND CONCLUSIONS

An investigation of snap load behavior in marine cable systems was approached using simple and complex dynamic models. Based upon the simple dynamic model, three dimensionless groups were identified which are useful for understanding snap load phenomena. A design

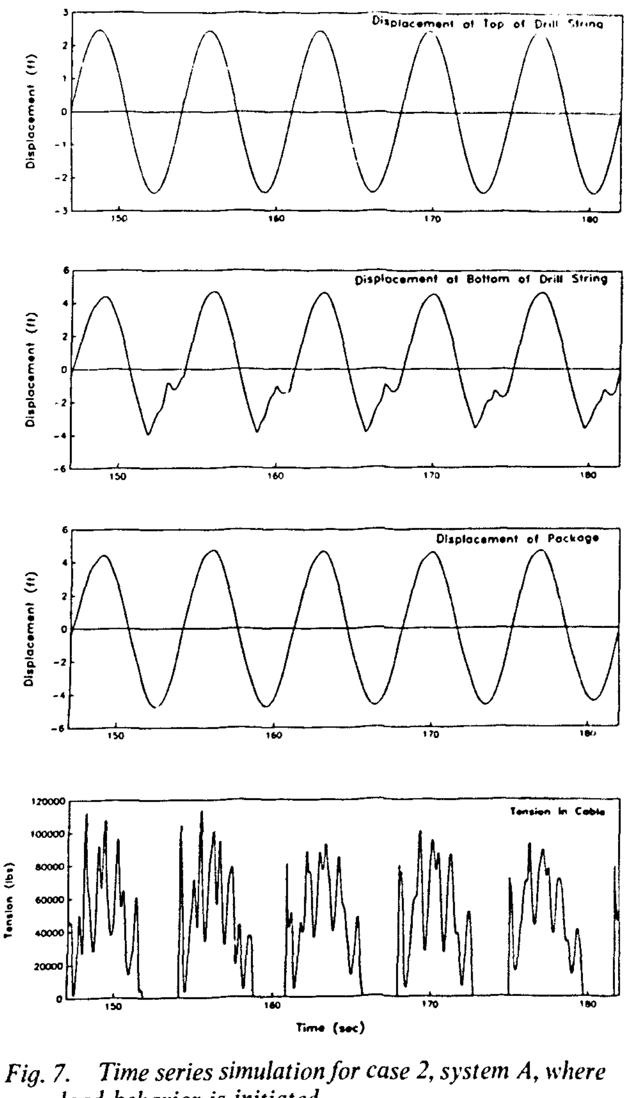

Fig. 7. Time series simulation for case 2, system A, where snap load behavior is initiated

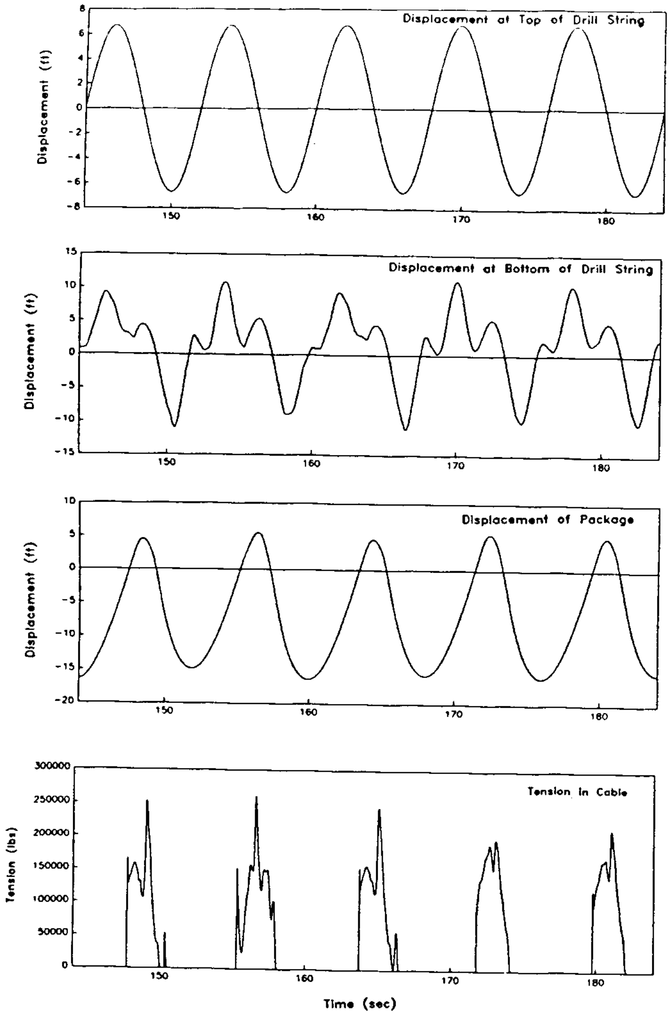

Fig. 8. Time series simulation for case 3, system A, where significant snap load behavior occurs

curve approach was presented which provides the offshore engineer with a preliminary means to determine whether slack cable conditions will occur for a particular design. The simple dynamic model should be used both to provide qualitative information about the behavior of a marine cable design and as a guide to when a more detailed dynamic analysis is needed. For designs which are clearly in the taut regimes, one may elect to refine the design without resorting to a time domain simulation. However, if it is in or close to the slack regime *a* the use of a more complex dynamic model is warranted. This would allow the engineer to more accurately evaluate the dynamic behavior of the marine cable system and to analyze snap load behavior in terms of its magnitude and duration. This two-part analysis approach and the dimensionless parameters can be used for non-marine applications.

From the SDOF model of the cable/package system, the pertinent design variables and the relative importance of each of the variables was determined. The most important parameters were found to be the ratio of the structural mass to the virtual mass of the package and the directional characteristics of the vessel heave response amplitude operator. It was found that the drag coefficient is not as important as the coefficient of hydrodynamic added-mass. This result reinforced the need to accurately evaluate the hydrodynamic properties of the package since, the virtual mass is the sum of the package mass and the added-mass. The experiments reported here illustrate that the use of common analytical approximations are not accurate for complex and porus geometrical shapes. More laboratory testing is required to better understand this general class of porous bodies which are quite common in offshore applications. The vessel from which the marine cable system is suspended and its motion characteristics was shown to be capable of significantly mitigating or accentuating the occurrence of snap loads. Based upon this and previous studies[6], it is clear that heave compensation could be used to overcome poor heave motion characteristics of the floating platform.

The cases which were studied were subjected to moderate design wave conditions and the magnitude of the snap loads was observed to be within tolerable design limits, i.e. the tension loading was below the estimated break strength of the cable system. In these cases it was observed that there are clear patterns to the timing of the snap loads and that it should be possible to sustain one or more snap load cycles without the cables breaking. These snap load cycles can be expected to reduce the useful life of the cable components of the system, but the results indicate that successful placement or retrieval of a package from the seafloor could be achieved while sustaining some level of snap loads in the system.

ACKNOWLEDGEMENTS

The authors gratefully acknowledge the support of the Ocean Drilling Program during this study. In particular, the authors would like to thank Mr. Barry Harding and Mr. Steve Howard to their helpful discussions on the design and deployment of the hard rock drilling base.

REFERENCES

1 Goeller, J. E. and Laura, P. E. Analytical and experimental study of the dynamic response of segmented cable systems, *J. Sound and Vibration*, 1971, **18**(3), 311–329

2 Liu, F. C. *Snap Loads in Lifting and Mooring Cable Systems Induced by Surface Wave Conditions*, NCEL Technical Note N-1288, Port Hueneme, CA, Sept. 1973

3 Yoshida, K. and Oka, N. Snap loads in taut moored platforms, *J. Soc. Naval Arch. Japan*, 1978, **144**, 205–213

4 Rabinowitz, P. D., Carlson, R., Garrison, L., Gartner, S., Herrig, S., Massullo, J. and Merrell, W. J. The ocean drilling program: The next phase in scientific ocean drilling, *Offshore Technology Conference*, 1984, 4989, 279–286

5 Niedzwecki, J. M. and Harding, B. W. ODP drill string analysis capabilities, *Deep Offshore Technology Conference*, Monte Carlo, 1987, 1, 78–97

6 Niedzwecki, J. M. and Thampi, S. K. Heave compensated response of long multi-segment drill strings, *J. Applied Ocean Research*, 1988, **10**(4), 181–190

7 Tse, F. S., Morse, T. E. and Hinkle, R. T. *Mechanical Vibrations*, Allyn and Bacon, Inc., Boston, MA, 1978

8 Goeller, J. E. and Laura, P. E. A theoretical and experimental investigation of impact loads in stranded steel cables during longitudinal excitation, *Proc. 5th Southeastern Conf. Theor. and App. Mech.*, N. Carolina State Univ. and Duke Univ., 1970

9 Iwan, W. D. Dynamic response of suspended underwater systems, *J. Acoustical Soc. America*, 1972, **51**(5) (Part 2), 1688–1696

10 Niedzwecki, J. M. and Serocki, S. T. Drill string sensitivity to hydrodynamic approximations, *Proc. Oceans '85*, Marine Technology Society, Vol. 1, 1985

11 Deep Sea Drilling Project, *Computer Analysis and Field Measurement of Stress in Long Drill Strings Suspended form A Floating Vessel*, Technical Report No. 22, July 1984

12 Newmark, N. M. A method of computation for structural dynamics, *ASCE Transactions*, 1962, 127, 1406–1435

13 Basu, A. K. and Dutta, A. Dynamic behavior of guyed towers, *Third Intl. Conf. Behavior of Offshore Structures*, MIT, Cambridge MA, 1982, 529–454

14 Kennard, E. H. *Irrotational Flow of Frictionless Fluids, Mostly of Invariable Density*, David Taylor Model Basin Rpt. 2299, Washington D.C., 1967